Understanding the Influence of Receptor Transport on Nanoparticle-Cell Interactions

Dexter Theisen

Under the direction of

Prof. Qin Qi
Dr. Keng Wai Chan

Department of Chemical Engineering
Massachusetts Institute of Technology

Research Science Institute
Final Paper
August 4, 2026

Abstract

Nanoparticles are premier candidates for targeted drug delivery, yet their ability to alter host cell mechanics remains a critical, multiscale biophysical challenge. Despite even low surface concentrations, nanoparticles can induce non-trivial effects, occasionally leading to adverse cellular outcomes such as membrane rupture. Building on the recent identification of a critical length scale explaining particle-induced membrane tension, this study introduces an advanced model that combines membrane mechanics with receptor-mediated binding and configurational entropy associated with receptor redistribution. This coupled approach allows us to map equilibrium wrapping regimes and evaluate the performance of nanoparticles featuring ligands. The introduction of receptor-transport does significantly change the model's output, with wrapping angles at steady state shifting by as much as 0.15π. Ultimately, these insights establish a predictive computational framework for optimizing particle design and selection, paving the way for safer, more successful nanomedicines.

Summary

The effectiveness of targeted drug delivery is strongly influenced by how nanoparticles interact with cellular membranes. Therapeutic compounds carried by nanoparticles are formulated to either adhere to or be internalized by specified cells. However, nanoparticle–cell interactions are complex, multiscale biophysical processes, making them challenging to model. Existing frameworks assume coarse simplifications, such as fixing membrane tension as constant, even though particle-induced deformation causes it to vary. As such, the discrepancies between empirical and simulated results are large, with some linear models failing to reproduce experimentally observed concentration-dependent adsorption. Recent work, however, has developed an improved model that predicts a more accurate adsorption isotherm and identifies a critical length scale d_c, below which membrane tension mediates effects from nonadjacent particles: as one particle adsorbs, it deforms the membrane, increasing the tension and making it harder for other local and nonlocal particles to adsorb as well. The model predicts a nonlinear adsorption isotherm, whereas previous models (that assume particles are always independent) incorrectly predict near-linear behavior. Previous work determines equilibrium configurations by minimizing the total free energy of the system, consistent with classical thermodynamics. The work we present in this study revises the governing free-energy functional to explicitly account for membrane-bound receptors and particle ligands. As a ligand-coated particle adheres to the cell membrane through receptor–ligand binding, it recruits mobile receptors, causing them to accumulate around the contact region. This rearrangement reduces the configurational entropy of the receptors and therefore incurs an entropic penalty that we incorporate into our governing energy equation. Using our model, we find that the introduction of receptor configurational entropy reduces the effective adhesion strength; as receptor availability decreases relative to ligand density, the partial wrapping equilibrium shifts towards smaller wrapping angles by up to 0.15π, and completely wrapped states exist under a smaller range of conditions. These results demonstrate that receptor-ligand interactions must be considered jointly when predicting adsorption, and that our model provides a more physically complete description of nanoparticle interaction with the cell membrane.

1 Introduction

Nanoparticles are vital for various biomedical technologies, such as targeted therapeutics [1] and diagnostic imaging [2]. In many of their applications, a key interaction is that with the cell membrane [3]. Nanoparticles may need to be partially wrapped (e.g. drug carriers adhering to red blood cells), be engulfed fully, or resist detachment under physiological forces (e.g. shear from the bloodstream) depending on intended function [4, 5]. As such, the effectiveness of nanomedicines is determined both by the compounds they carry and by their interaction dynamics. Engineering this problem is difficult because nanoparticle behavior is governed by a large design space: the kinetics depend on particle size, ligand density, adhesion strength, as well as other physicochemical properties [6, 7]. Likewise, surface tension, bending modulus, receptor density, and other membrane variables also have effects on the equilibrium states. Further, all the aforementioned parameters are not necessarily monotonic [6, 7]. For example, stronger adhesion may promote uptake, but can also boost membrane tension, inducing cell stiffening and unwanted lysis. As a result, empirical optimization alone leaves large regions of the multidimensional design space unexplored, motivating the computational, predictive model this paper proposes [8].

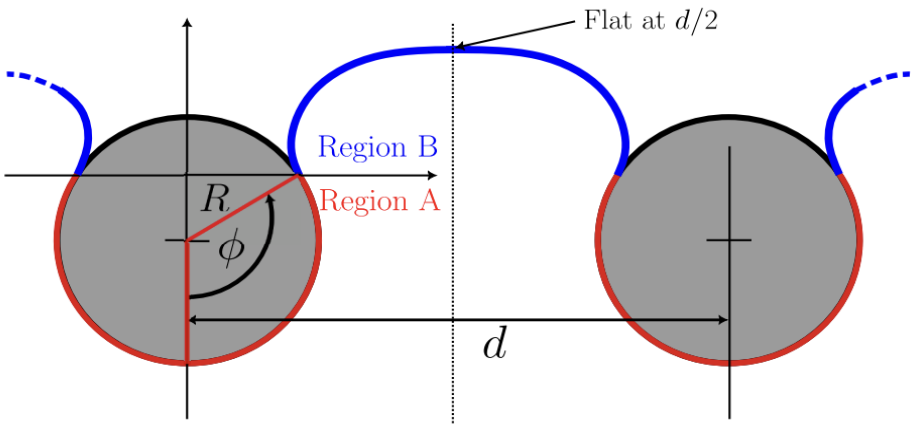


Figure 1: Schematic illustration of a nanoparticle–membrane system. The section of the membrane (in red) that the spherical particle (in gray) is contacting is denoted as region A, and the section (in blue) that the particle is not contacting is denoted as region B [7].

Previous work has developed a model that predicts the adsorption, uptake, and detachment of spherical nanoparticles interacting with a finite lipid membrane [7]. (Our work retains the restriction to spherical nanoparticles because they provide a simple, symmetric geometry that retains key behavior while drastically simplifying calculations and computational resources. Furthermore, spheres are actually a reasonable first-order representation of nanoparticles like gold and silica that are used in numerous experiments [9].) The surface area in the "particle-bound" region A is denoted as S_A and the surface area in the "particle-free" region B is denoted as S_B. Within Pincus & Qi's framework, the equilibrium configurations are determined by minimizing a free-energy functional comprising stretching, bending, and adhesion contributions. By enforcing lipid conservation to maintain physical consistency (as under the timescale studied, the lipid bilayer does not lose or gain lipid matter), the model allows membrane tension to change in response to particle-induced deformation. This consideration revealed interactions—previously ignored by fixed-tension models—between spatially separated particles that exist even at very dilute concentrations [7]. Specifically, as one particle is being adsorbed, it changes the tension of the membrane (both locally and non-locally), influencing the energies required for other nonadjacent particles to adsorb; this phenomenon is known as "particle coupling" [7]. Yet, Pincus & Qi's work uses a nonspecific adhesion-energy density, modeling adhesion as an effective, spatially uniform attraction between a particle and a membrane. Many biomedical nanoparticles, however, are functionalized with surface ligands that bind selectively to receptors on the cell membrane, rendering a uniform affinitive force as physically inaccurate [6, 10]. In these systems, particle-mediated wrapping is instead governed jointly by receptor-ligand binding along with membrane deformation. Receptor-ligand bond formation attracts receptors to the particle-bound region, while configurational entropy penalizes deviations from an initially uniform distribution (discussed more in 3.2). This work, performed by Gao et al., accounts for receptor-diffusion but does not consider the particle coupling that Pincus & Qi do [6]. Hence, in this paper, we propose a free-energy functional that synthesizes the Gao et al. and Pincus & Qi frameworks to explicitly account for the

specific and entropic effects of receptor-ligand binding while simultaneously incorporating the principle of deformation-dependent membrane tension.

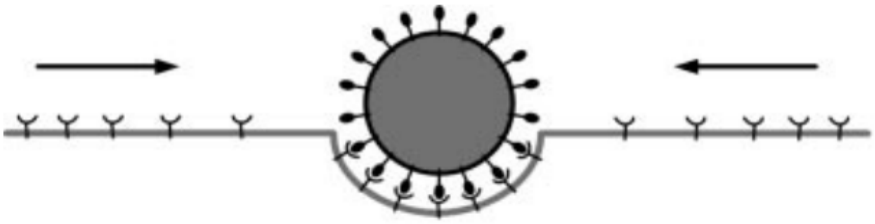


Figure 2: Schematic illustration of a receptor-ligand interaction. Receptors on the membrane are diffusing from an initially uniform concentration (observed primarily at the edges) to the particle-contact region in order to form bonds with particle ligands [6].

2 Methodology

We begin by defining the geometry of an adhering particle. The first variable to motivate is ϕ, the wrapping angle (see Figure 2), which describes how far the membrane has enveloped the particle; mathematically, ϕ represents the angle of the arc produced in region A by particle deformation. Following previous work, to understand the equilibrium configurations for a given particle-membrane system, we plot the free-energy of the system as a function of ϕ [7]. The equilibrium regime is then determined by the minima of this energy landscape, $E(\phi)$. We denote an unwrapped or free state at $\phi = 0$ by F, a partially wrapped state at $0 < \phi < \pi$ by P, and a completely wrapped state at $\phi = \pi$ by C. A single letter indicates that only one stable state is possible. When two minima exist, the first letter denotes the global minimum (stable state) and the subscript denotes the additional local minimum (metastable state). This convention produces six observed regimes, $F, F_C, F_P, P_C, C_P,$ and C.

Figure 3 graphs the free-energy versus wrapping angle for 5 different concentrations of nanoparticle, color-coded according to the legend. Minima points are indicated and are used to determine the appropriate regime, which also appears in the legend.

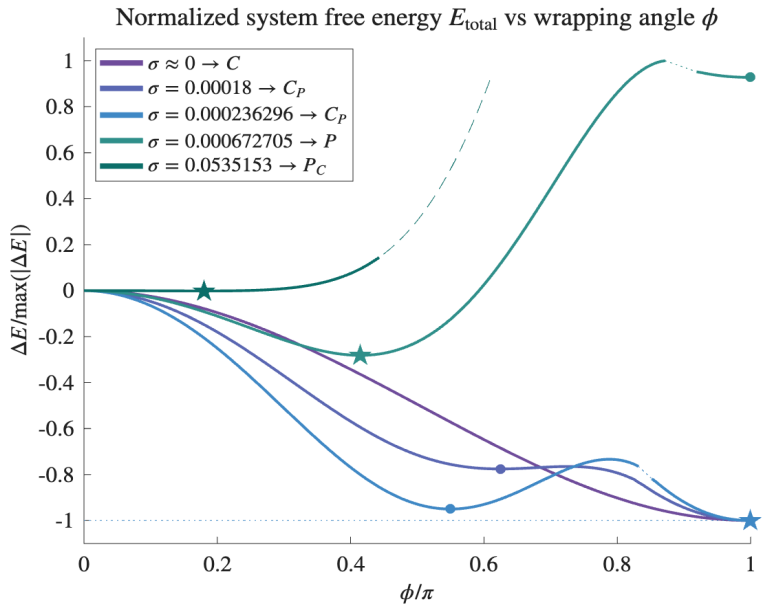


Figure 3: Normalized system energy as a function of ϕ for different values of σ. Stars indicate global minima, and dots indicate local minima. $R = 50\,\text{nm}$, $\kappa = 10^{-19}$ J, $k_D = 0.30$ pJ μm^{-2}, $\zeta = 10^{-3}$, $\alpha_i = 10^{-5}$, $T = 300\,\text{K}$. See Table 2 for definitions of variables. Regenerated from [7].

Previous work uses the following functional, which comprises stretching, bending, and adhesion energy components [7]:

$$E_{\text{total}} = E_{\text{stretch},A} + E_{\text{stretch},B} + E_{\text{bend},A} + E_{\text{bend},B} + E_{\text{adhesion}} \tag{1}$$

Importantly, this framework assumes that nanoparticle-membrane binding is nonspecific. However, as discussed above, many nanomedicines feature ligands and real membranes have receptors; accordingly, we seek to model their interactions [6] in order to improve the physical accuracy of our model. We introduce two main updates to current modeling efforts: (1) an updated definition for the adhesion energy that is specific in terms of receptor-ligand bonds and (2) an entropic energy contribution associated with the configurational redistribution of mobile receptors along the cell membrane. (Receptors are mobile because the lipid bilayer and proteins are held together by noncovalent bonds, allowing lateral diffusion in a manner similar to fluids [11].) We assume one-to-one receptor-ligand binding in region A: ξ_0 is the initial uniform receptor areal density, ξ_L is the bound-receptor areal density (equal to the

ligand density), and $\xi(\mathbf{x})$ is the free-receptor areal density in region B. The quantity $E_{\mathrm{RL}} > 0$ denotes the magnitude of the receptor–ligand bond energy. Our new functional is then the sum of the following constituent expressions:

$$\begin{aligned} E_{\mathrm{total}} = & \underbrace{-\xi_L E_{\mathrm{RL}} S_A}_{E_{\mathrm{adhesion}}} + \underbrace{\frac{k_D}{2}\frac{\alpha_A^2}{1+\alpha_A} S_A}_{E_{\mathrm{stretch},A}} + \underbrace{\frac{k_D}{2}\frac{\alpha_B^2}{1+\alpha_B} S_B}_{E_{\mathrm{stretch},B}} \\ & + \underbrace{\xi_L \ln\left(\frac{\xi_L}{\xi_0}\right) k_{\mathrm{B}} T S_A}_{E_{\mathrm{entropy},A}} + \underbrace{\int_{S_B} \xi(\mathbf{x}) \ln\left(\frac{\xi(\mathbf{x})}{\xi_0}\right) k_{\mathrm{B}} T \, \mathrm{d}S}_{E_{\mathrm{entropy},B}} \\ & + \underbrace{4\pi\kappa\,(1-\cos\phi)}_{E_{\mathrm{bend},A}} + \underbrace{\pi\kappa \int_0^{s_{\mathrm{end}}} \frac{p_\psi^2}{4r} \, \mathrm{d}s}_{E_{\mathrm{bend},B}}, \end{aligned} \tag{2}$$

with all constants and variables defined in Table 2. Each contribution is physically motivated and consistent with previous literature. Membrane stretching is modeled as Hookean area dilation, while membrane bending is described by the Helfrich curvature free-energy functional [12, 13]. Adhesion and entropy calculations are developed in sections 3.1 and 3.2 respectively.

Wrapping morphs the membrane, but like in Pincus & Qi [7], under the timescale considered in this paper, this process neither creates nor destroys lipids. As such, although regions A and B may change their area via stretching, the sum of their corresponding unstretched areas must equal that of the initial membrane area, S_0. Similarly, receptor-ligand interactions may redistribute the positions of receptors, but the overall population remains fixed. Thus, subject to the constraints of lipid and receptor conservation, we minimize the total energy of the system using the updated equations above.

$$\frac{S_A}{1+\alpha_A} + \frac{S_B}{1+\alpha_B} = S_0 \qquad , \qquad \xi_L S_A + \int_{S_B} \xi(\mathbf{x}) \, \mathrm{d}S = \xi_0 S_0 \tag{3}$$

(See Table 2 for definitions of relavent variables.)

This equilibrium problem is solved as a nested calculation. For each of the (linearly-spaced) 150 wrapping angles $\phi \in [0.01°, 179.9°]$ for which we minimize E_{total} over the two stretch

variables (α_A, α_B) in order to plot Figure 3, we use MATLAB's `fmincon` routine with the SQP algorithm (optimality, constraint, and step tolerances are all chosen to be 10^{-12}). Each evaluation of E_{total} requires the shape of the particle-free membrane, which is itself the solution of a boundary-value problem. Specifically, we solve the (axisymmetric) Helfrich shape equations subject to tangential contact with the particle (at $r = R\sin\phi$) and a far-field flat boundary (at $r = d/2$). This innermost sub-problem is the dominant computational cost and is handled by the look-up table described below. Successive ϕ are solved by continuation: the optimal (α_A, α_B) at one angle are used to calculate the next, with the first angle initialized from analytic estimates.

$\Delta S_B/R^2$, the excess area of the deformed particle-free region, is used to calculate the region B stretching energy, the global area constraint, and receptor conservation equations. Together with $E_{\text{bend},B}$, we are then able to calculate E_{total}. Therefore, we desire to solve for both these values. Importantly, $\Delta S_B/R^2$ and $E_{\text{bend},B}/\pi\kappa$ depend only on $\left(\bar{\Sigma}_B = \Sigma_B R^2/\kappa,\ \phi,\ d/R,\ \bar{q}\right)$, where $\bar{q} = \frac{q_B R^2}{\kappa} = \frac{\xi k_{\text{B}} T \ln(\xi/\xi_0) R^2}{\kappa}$ with q_B representing the region B entropy energy density. Thus, we precompute both quantities on a fixed grid of $800 \times 200 \times 67 \times 32$ nodes, spanning $\bar{\Sigma}_B \in [10^{-5}, 10^{8}]$ logarithmically, $\phi \in (0, \pi)$ with smoothstep clustering near the endpoints, $d/R \in [3, 10^{5}]$ logarithmically, and $\bar{q} \in [-8, -8 \times 10^{-6}] \cup \{0\}$ logarithmically. The tabulated fields are stored as quadrilinear `griddedInterpolant` objects and queried inside the objective function, reducing the computational cost of each energy evaluation from solving an ODE to simply interpolating. The median error for interpolation queries (compared interpolation values at 10^5 random test points to their corresponding values from solving the ODE) is 5×10^{-8}, a residual that is far below the precision at which E_{total} is calculated.

Wrapping regimes are assigned from the topology of the $E(\phi)$ landscape. The data are fitted with a smoothing spline (`csaps`, smoothing parameter $1 - 10^{-5}$) and resampled at 10^4 points, from which interior local minima and maxima are extracted with `islocalmin`/`islocalmax`.

3 Results & Discussion

3.1 Updated Adhesion Expression

In order to incorporate receptor-ligand binding into the finite-membrane framework, we reformulate the adhesion energy in terms of the density of bound receptors (ξ_L) and the energy of each receptor-ligand bond (E_{RL}), instead of an effective nonspecific adhesion parameter [7]. This update combines the receptor-transport model of Gao et al. [6] with the stretching and membrane-deformation contributions of the Pincus & Qi model [7]. Further, it allows the adhesion term to be coupled directly to the receptor-conservation condition introduced in this work. Two similar receptor-based adhesion expressions were considered. The first assumes the number of receptor-ligand bonds scales with the instantaneous (currently deformed) area of the particle-bound region:

$$E_{\mathrm{adhesion}}^{inst} = -\xi_L E_{\mathrm{RL}} S_A. \tag{4}$$

The second preserves the receptor count from the initially unstretched membrane area:

$$E_{\mathrm{adhesion}}^{init} = -\xi_L E_{\mathrm{RL}} \frac{1+\alpha_i}{1+\alpha_A} S_A. \tag{5}$$

The two expressions differ only by the factor $\frac{1+\alpha_i}{1+\alpha_A}$, and therefore converge as $\alpha_A \to \alpha_i$.

We compared the two expressions for parameter sets of $\{\varepsilon,\ n_0,\ d,\ R,\ k_D,\ \kappa,\ \alpha_i\}$ over wrapping angles ranging from 15° to 180° and d values ranging logarithmically from 0.3831μm to 2802.5μm. Across all tested values of ϕ, the relative difference remained between approximately -0.6% and -0.1% (implying that α_A changes on a relatively small scale). Thus, the initial-area expression produced an adhesion energy only slightly smaller in magnitude than the instantaneous-area expression and these results indicate that the two expressions are effectively interchangeable. To maintain consistency with the receptor conservation equation, the subsequent analysis uses Eq. 5.

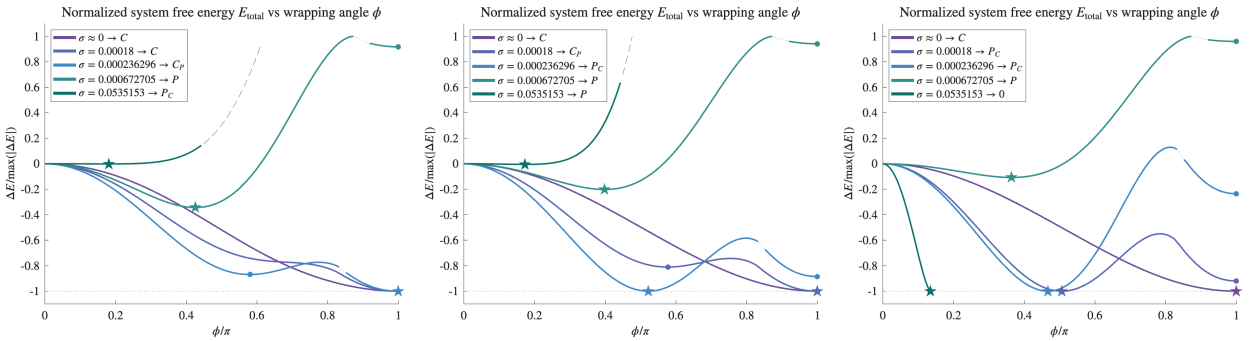
3.2 Entropy

The density of ligands in nanoparticle-membrane systems is typically much greater than that of receptors [6]. (The precise ratio of receptors to ligands is defined by $\bar{\xi} = \frac{\xi_0}{\xi_L}$.) As such, because the model calls for one-to-one binding, every ligand in the bound region must be matched with a receptor [6]. Yet, $\xi_L \gg \xi_0$, meaning that receptors need to move into the particle-contact region (as displayed in Figure 2) [6]. Importantly, every receptor drawn beneath the particle is removed from a nearly uniform space, and this process is associated with a configurational entropy term that opposes the redistribution. With the initial-area convention, the bound-region contribution is $E_{\text{entropy},A} = \xi_L \ln(\xi_L/\xi_0) k_{\text{B}} T S_A$, derived in [6] by treating mobile receptors as similar to an ideal two-dimensional gas. Each captured receptor gains E_{RL} from binding but loses $k_B T \ln \frac{\xi_L}{\xi_0}$ from configurational entropy. Hence, combining this term with the adhesion term of Eq. 5 gives the effective adhesion energy density, which represents the net free-energy decrease per unit area of new contact.

$$w_{\text{eff}} = \xi_L \left(E_{\text{RL}} - k_{\text{B}} T \ln \frac{\xi_L}{\xi_0} \right) \tag{6}$$

so that $E_{\text{adhesion}} + E_{\text{entropy},A} = -w_{\text{eff}} S_A$. The limit $\bar{\xi} \to 1$ can be used to anaylze the accuracy of the model, as at $\bar{\xi}$ the entropic penalty should vanish and correctly produces the results of Pincus & Qi's entropy-free model.

Figure 4 sweeps $\bar{\xi}$ over a range for fixed parameters (see Table 2); moving right, the ratio decreases, meaning there is a larger disparity in the density of receptors versus ligands. As a result, the entropy penalty increases, shifting the equilibrium states significantly. Panel (a) sets $\xi_0 = \xi_L$, so every entropy term is zero by construction and the landscape of previous work is reproduced almost identically (a small region B effect exists) [7]; panels (b) and (c) then increase the penalty to $2.30 k_{\text{B}} T$ and $4.61 k_{\text{B}} T$ per receptor (values given by $\ln(1/\bar{\xi})$). Two distinct effects can be separated.



(a) $\bar{\xi} = 1$ (b) $\bar{\xi} = 0.1$ (c) $\bar{\xi} = 0.01$

Figure 4: Normalized system energy as a function of ϕ for the same five nanoparticle surface fractions σ at three receptor contrasts: (a) $\bar{\xi} = \xi_0/\xi_L = 1$, for which the entropy vanishes and the entropy-free landscapes of Figure 3 are recovered identically; (b) $\bar{\xi} = 0.1$; and (c) $\bar{\xi} = 0.01$. Stars indicate global minima, dots indicate local minima, and each curve is normalized by its own $\max(|\Delta E|)$.

The inclusion of the entropy term progressively destabilizes complete wrapping relative to partial wrapping. At $\sigma = 2.36 \times 10^{-4}$ (the sky blue line in Figure 4), the fully wrapped state changes from the global minimum at $\bar{\xi} = 1$ (C_P), to a metastable state at $\bar{\xi} = 0.1$ (P_C), and finally rises above the flat reference at $\bar{\xi} = 0.01$, where $\Delta E/\max(|\Delta E|)$ increases from -0.68 to $+0.28$. Complete wrapping is therefore no longer viable, even as a metastable state. Accordingly, the surface fraction at which complete wrapping is lost decreases from between 2.4×10^{-4} and 6.7×10^{-4} at $\bar{\xi} = 1$, to between 1.8×10^{-4} and 2.4×10^{-4} at $\bar{\xi} = 0.1$, and to below 1.8×10^{-4} at $\bar{\xi} = 0.01$.

Second, the partial minima move towards lower ϕ monotonically, as summarized in Table 1. They shift by 0.08π–0.15π across the tested range, with the largest changes occurring near phase boundaries (often changing the global equilibrium from a complete to a partial state).

σ	$\bar{\xi} = 1$	$\bar{\xi} = 0.1$	$\bar{\xi} = 0.01$
1.80×10^{-4}	0.62 (C_P)	0.56 (C_P)	0.47 (P_C)
2.36×10^{-4}	0.57 (C_P)	0.53 (P_C)	0.47 (P_C)
6.73×10^{-4}	0.43 (P_C)	0.40 (P_C)	0.38 (P_C)
5.35×10^{-2}	0.19	0.18	0.14

Table 1: Location (ϕ/π normalized) of the deepest partial well in Figure 4.

For the following phase diagrams, we use the receptor-mediated adhesion strength $|\bar{w}| = |2\xi_L E_{\text{RL}} R^2/\kappa|$ and the initial membrane tension $\bar{\Sigma}_i = \Sigma_i R^2/\kappa$.

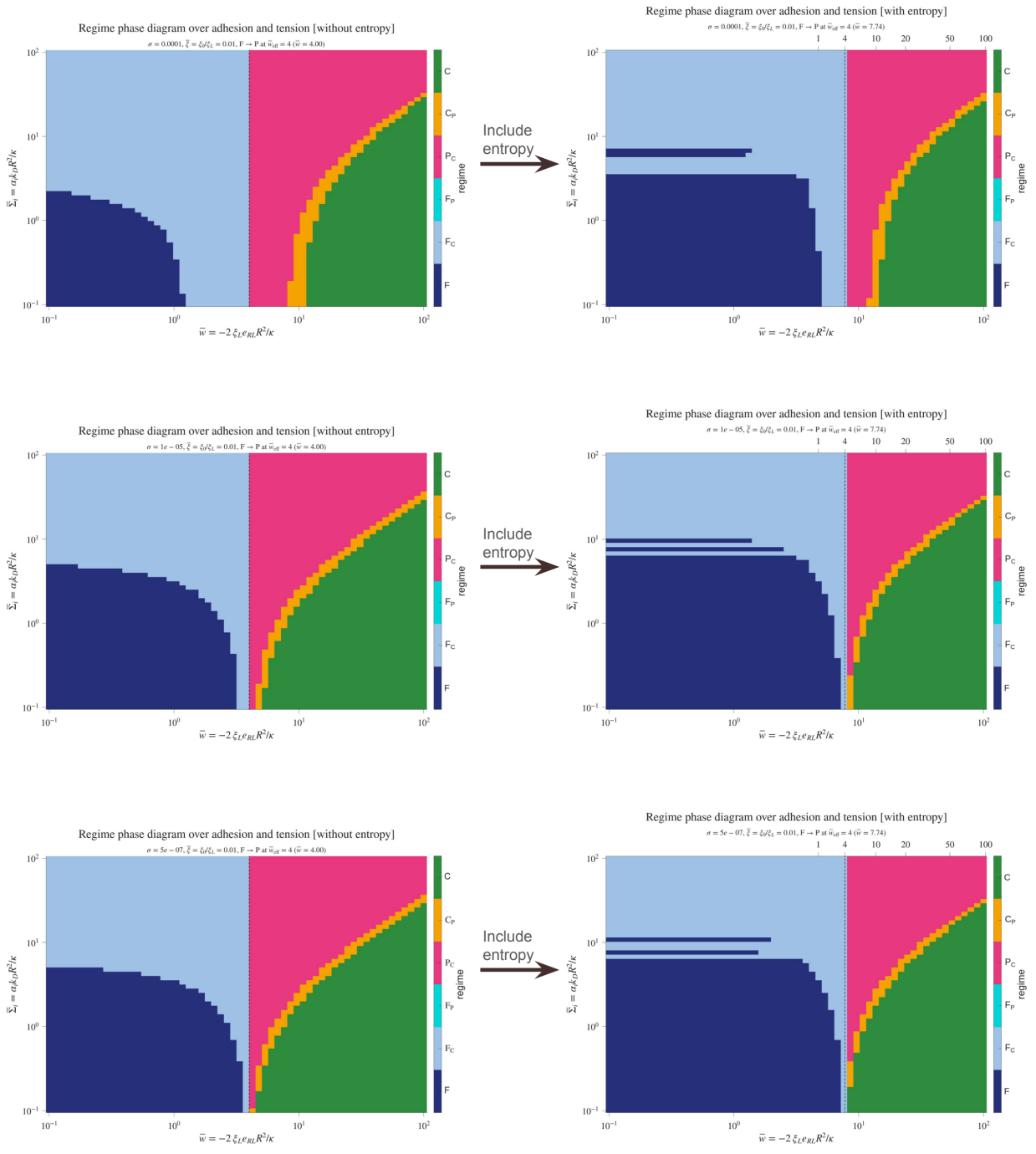


Figure 5: Wrapping-regime phase diagrams in the $(\bar{w}, \bar{\Sigma}_i)$ plane at $\sigma = 1 \times 10^{-4}$ (top pair), $\sigma = 1 \times 10^{-5}$ (middle pair), and $\sigma = 5 \times 10^{-7}$ (bottom pair) values. Left column plots do not incorporate entropy terms into their free-energy equation. Right column plots do incorporate entropy terms into their free-energy equation with $\bar{\xi} = 0.01$.

Figure 5 summarizes the effect of entropy on the global phase behavior. Because the entropic penalty scales with S_A, Eq. 6 predicts an approximately uniform shift along the

adhesion axis of

$$\Delta\bar{w} = \frac{2\xi_L \ln(1/\bar{\xi}) k_B T R^2}{\kappa} = 4.8 \quad (\bar{\xi} = 0.01) \tag{7}$$

This moves the free-to-wrapped transition from $\bar{w} = 4$ to approximately 8.8. However, the measured shift is slightly smaller than 4.8 because the negative free-region B entropy partially offsets the bound-region penalty. The complete-wrapping boundary shifts similarly: at $\sigma = 5 \times 10^{-7}$, the C region reaches $\bar{\Sigma}_i \approx 1$ near $\bar{w} \approx 8$, rather than $\bar{w} \approx 4$. It can be observed that entropy has its greatest effect at weak adhesion, and becomes less important as $\bar{w}$ increases. Most importantly, it increases the parameter space for which particles remain completely unbounded and deceases the parameter space for which they remain completely engulfed, as well as simply reduces the wrapping angle for partially adhered states.

It is also important to address the artifacts in Figure 5: the gridded interpolation table was built with a shooting solver, which fails near complete wrapping because the contact line radius $R \sin\phi$ collapses as $\phi \to \pi$, leading to some F cells being incorrectly labeled as F_C. Though beyond modeling, this error is arguably practically insignificant, as only the right-hand side of the phase diagrams proves relevant to drug design.

4 Conclusion & Future Work

In this work, we incorporated receptor-ligand binding and configurational entropy into a model of nanoparticle wrapping. Reformulating the adhesion energy in terms of the receptor-ligand bonds from the instantaneous versus initial membrane area only shifted values by $\sim 0.1\%$–0.6%. By contrast, introducing receptor entropy substantially altered the system's energy landscape, shifting the locations of partial minima by $\sim 0.08\pi$–0.15π, expanding the range of conditions under which particles remain unbound. These results show that receptor availability and ligand density should therefore be treated as design variables for creating nanomedicines, given the significant affect they have on equilibrium states. However, a greater number of ligands does not simply translate into a proportional increase in adhesion strength,

because of the incurred entropic penalty. This distinction has practical implications for targeted drug engineering, as the same ligand-functionalized particle may exhibit different adsorption behavior across cell types with different receptor densities. As such, the computational model established in this paper provides a framework to predict equilibrium states and wrapping regimes for different formulations of nanomedicines, in order to improve their efficacy and decrease the reliance on empirical testing. The next steps of this work are to generate figures that compare predicted adsorption isotherms, as well as the kinetics of adsorption as a function of time, to data from empirical studies. Previous work already captures the sublinear behavior of adsorption, but the predicted bounds still deviate slightly from the experimental range [7]. Our goal is to update these bounds so that they more accurately capture the multiscale biophysical dynamics. Ultimately, incorporating receptor-mediated binding and configurational entropy into a computational model has significant effects, and may help inform the design of nanomedicines for desired adhesion and internalization outcomes.

5 Key Takeaways

- Replaced the nonspecific adhesion parameter with an explicit receptor-ligand model; very small effect (0.1%–0.6%).
- Receptor redistribution imposes an entropic penalty of $k_B T \ln(1/\bar{\xi})$ per receptor. This penalty shifts the equilibrium states, as described by the phase diagrams. Specifically, partial-wrapping minima move toward smaller wrapping angles by approximately 0.08π–0.15π, and the range of conditions under which particles remain unbound increases.
- Given how much the addition of entropy changes the energy landscape, we conclude nanoparticle wrapping cannot be predicted from stretching, bending, and adhesion energy alone. Hence, receptor mechanics (specifically configurational entropy) must be considered jointly when designing particles for specific surface adhesion or complete internalization tasks.

6 Acknowledgments

I would like to thank Prof. Qin Qi and Dr. Keng Wai Chan for their invaluable mentorship on this project. I am grateful to my RSI tutor, DJ Liveoak, for his prudent guidance and continued support. I would also like to thank my last week TA, Scarlet Gitelson, and my "nobody", Emmanuel Soon Yi En, for the extremely helpful feedback they provided in their reviews of my paper. I am deeply grateful to Mr. George Ho, Mrs. Andrea Ho, and Mr. Jonathan A. Marcus for generously sponsoring my enrollment in the Research Science Institute, as well as to the Center for Excellence in Education and the Massachusetts Institute of Technology for making this experience possible. I sincerely appreciate my parents for always supporting my goals. I acknowledge the MIT Office of Research Computing and Data for providing high performance CPU resources that were used to generate the results reported within this paper. Finally, I would like to thank my fellow RSI students, whose inquisitiveness, generosity, and collaborative spirits have made the program an intellectually vibrant and deeply rewarding experience.

Generative AI Statement

Generative AI was used to assist with formatting Table 2 in the appendix of the paper, as well as with transcribing handwritten notes into LaTeX format. Generative AI was used to help modify MATLAB code so it could be executed in parallel on MIT ORCD's *Engaging* cluster.

References

[1] J. Shi, P. W. Kantoff, R. Wooster, and O. C. Farokhzad. Cancer Nanomedicine: Progress, Challenges and Opportunities. *Nature Reviews Cancer*, 17(1):20–37, 2017.

[2] J. Estelrich, M. J. Sánchez-Martín, and M. A. Busquets. Nanoparticles in Magnetic Resonance Imaging: From Simple to Dual Contrast Agents. *International Journal of Nanomedicine*, 10:1727–1741, 2015.

[3] R. B. Huang, S. Mocherla, M. J. Heslinga, P. Charoenphol, and O. Eniola-Adefeso. Dynamic and Cellular Interactions of Nanoparticles in Vascular-Targeted Drug Delivery. *Molecular Membrane Biology*, 27(7):312–327, 2010.

[4] A. C. Anselmo, V. Gupta, B. J. Zern, D. Pan, M. Zakrewsky, V. Muzykantov, and S. Mitragotri. Delivering Nanoparticles to Lungs While Avoiding Liver and Spleen through Adsorption on Red Blood Cells. *ACS Nano*, 7(12):11129–11137, 2013.

[5] E. Chambers and S. Mitragotri. Long Circulating Nanoparticles via Adhesion on Red Blood Cells: Mechanism and Extended Circulation. *Experimental Biology and Medicine*, 232(7):958–966, 2007.

[6] H. Gao, W. Shi, and L. B. Freund. Mechanics of Receptor-Mediated Endocytosis. *Proceedings of the National Academy of Sciences of the United States of America*, 102(27):9469–9474, 2005.

[7] I. Pincus and Q. M. Qi. Nanoparticle-Induced Lipid Membrane Deformation Influences the Design of Biomedicine. *Biophysical Journal*, 125:1–12, 2026.

[8] Z. Zhao, A. Ukidve, V. Krishnan, and S. Mitragotri. Effect of Physicochemical and Surface Properties on In Vivo Fate of Drug Nanocarriers. *Advanced Drug Delivery Reviews*, 143:3–21, 2019.

[9] C. Contini, J. W. Hindley, T. J. Macdonald, J. D. Barritt, O. Ces, and N. Quirke. Size Dependency of Gold Nanoparticles Interacting with Model Membranes. *Communications Chemistry*, 3(1):130, 2020.

[10] S. Zhang, H. Gao, and G. Bao. Physical Principles of Nanoparticle Cellular Endocytosis. *ACS Nano*, 9(9):8655–8671, 2015.

[11] S. J. Singer and G. L. Nicolson. The Fluid Mosaic Model of the Structure of Cell Membranes. *Science*, 175(4023):720–731, 1972.

[12] E. A. Evans, R. Waugh, and L. Melnik. Elastic Area Compressibility Modulus of Red Cell Membrane. *Biophysical Journal*, 16(6):585–595, 1976.

[13] W. Helfrich. Elastic Properties of Lipid Bilayers: Theory and Possible Experiments. *Zeitschrift für Naturforschung C*, 28(11–12):693–703, 1973.

A Appendix

Table 2: Definitions of variables used in the nanoparticle-membrane energy model.

Symbol	Definition	Symbol	Definition
A	Particle-bound region of the membrane.	B	Particle-free region of the membrane.
E_{adhesion}	Membrane-particle adhesion-energy contribution.	E_{RL}	Binding energy of one receptor–ligand bond, 15 $\mathrm{k}_B T$.
ξ_L	Surface density (region A) of ligands on the particle, $5{\times}10^3/\mu m^2$	ξ_0	Initial membrane-uniform receptor density.
ξ	Local density of unbound receptors in region B.	R	Radius of the nanoparticle, 50 nm.
S_A	Membrane-particle contact area in region A, given by $S_A = 2\pi R^2(1-\cos\phi)$.	S_B	Surface area of the particle-free membrane region B.
$E_{\text{stretch},A}$	Membrane stretching energy contribution from region A.	$E_{\text{stretch},B}$	Membrane stretching energy contribution from region B.
k_{B}	Boltzmann constant.	T	Temperature, 300 K.
α_A	Fractional area increase of region A.	α_B	Fractional area increase of region B.
$E_{\text{entropy},A}$	Entropic contribution of the receptors in region A.	$E_{\text{entropy},B}$	Entropic contribution of the receptors in region B.
$E_{\text{bend},A}$	Membrane bending energy contribution from region A.	$E_{\text{bend},B}$	Membrane bending energy contribution from region B.
ϕ	Particle wrapping angle, with $0 \le \phi \le \pi$.	ψ	Angle between the membrane tangent and the radial r-axis.
p_ψ	Momentum conjugate to ψ, given by $p_\psi = 2r\dot{\psi} + 2\sin\psi$.	r	Horizontal distance from the membrane's axis of symmetry.
s	Arc-length coordinate along the region B.	s_{end}	Total arc length of region B (from contact to local flatness).
S_0	Unstretched area of the membrane (per particle), given by $\mathrm{S}_0 = d^2/(1+\alpha_i)$.	k_D	Dilatational modulus of the lipid bilayer, 0.3 $\mathrm{J/m^2}$.
α_i	Initial areal strain of the flat membrane, given by $\alpha_i = (\bar{\Sigma}_i\kappa)/(k_D R^2)$.	σ	Surface fraction representing effective concentration, given by $\pi R^2/d^2$.
κ	Bending modulus, $10^{-19}J$.	d	Effective center-to-center particle spacing.
w_{eff}	Effective adhesion-energy density after incorporating entropic penalty.	ζ	Dimensionless nonspecific adhesion strength relative to k_D, used in [7].
q_B	Region B receptor configurational entropy energy density, given by $\xi_B k_B T \ln(\frac{\xi_B}{\xi_0})$.	$\bar{q}$	Dimensionless region-B entropy parameter, given by $\bar{q} = \frac{q_B R^2}{\kappa}$
ΔS_B	Excess area of the deformed particle-free membrane.	Σ_i	Initial membrane tension.